DOI: 10.5281/zenodo.17338324

CHAPTER 15

Influence of Mn Doping on the Crystallinity and Morphology of Cerium Oxide Nanoparticles Synthesized by Co-precipitation

Nandkishor S. Sangle,[a]* Sangita S. Meshram[b]*

[a,b]*Physics Department, VPM'S B. N. Bandodkar College of Science (Autonomous), Building 6, Jnanadweepa, Chendani Bunder Road, Thane West, Thane 400601 Maharashtra, India*

Corresponding author Email: nssangle@vpmthane.org,[a] ssmeshram@vpmthane.org[b]

Received: 25 August 2025; Accepted: 13 October 2025; Available online: 13 October 2025

Abstract: In this study, we report the synthesis and characterization of pure cerium oxide (CeO_2) and manganese-doped cerium oxide (Mn–CeO_2) nanoparticles using the co-precipitation method. This synthesis route offers a simple and efficient pathway for obtaining high-purity nanomaterials. Structural and optical properties of the synthesized nanoparticles were analysed using X-ray diffraction (XRD), field emission scanning electron microscopy (FESEM), and UV-visible diffuse reflectance spectroscopy (UV-DRS). XRD analysis confirmed the formation of crystalline CeO_2 with a fluorite cubic structure, both in pure and Mn-doped samples. The incorporation of Mn did not alter the primary crystal phase but may have induced subtle lattice distortions. FESEM images revealed that the particle size ranges from

Materials Science: Advances in Synthesis, Characterization and Applications (Vol. 1) - Digambar M. Sapkal, Harshal M. Bachhav, Gaurav Mahadev Lohar, Sanjay P. Khairnar (Eds.)

ISBN: 978-93-95369-55-8 (paperback) 978-93-95369-46-6 (electronic) | © 2025 Advent Publishing.

https://doi.org/10.5281/zenodo.17338324

approximately 10 nm to 40 nm, indicating successful nanoscale synthesis. UV-DRS results demonstrated enhanced visible light absorption in Mn-doped CeO_2 compared to pure CeO_2, suggesting a narrowed bandgap and potential for improved photocatalytic performance. These findings highlight the influence of Mn doping on the structural and optical behaviour of cerium oxide nanoparticles.

Keywords: Cerium Oxide Nanoparticles, Mn-Doped CeO_2, Co-Precipitation Method, Structural Characterization, Optical Properties, XRD, UV-DRS, FESEM

1. Introduction

Cerium is a rare earth element and the second member of the lanthanide series in the periodic table. A defining feature of rare earth elements is the shielding of their 4f orbitals by outer 5p and 4d electrons, which imparts unique electronic and catalytic properties.[1] Unlike most lanthanides, cerium can exist in both +3 and +4 oxidation states,[2] enabling redox flexibility that is central to its catalytic functionality.

In bulk form, cerium oxide primarily exists as CeO_2 (cerium(IV) oxide) and Ce_2O_3 (cerium(III) oxide). However, at the nanoscale, cerium oxide nanoparticles (CeO_2 NPs) often contain a mixture of Ce^{3+} and Ce^{4+} ions, particularly on the surface, due to oxygen vacancies and surface defects. This mixed valence state is crucial to many of the material's exceptional properties. Cerium oxide nanoparticles have been widely investigated for a range of technological and biomedical applications. These include solid oxide fuel cells,[3] high-temperature oxidation-resistant coatings,[4] catalytic systems[5,6] solar energy devices[7] and potential pharmaceutical agents.[8] Among these, their most prominent application lies in catalysis, where their redox behavior and oxygen storage capacity (OSC) make them ideal materials. CeO_2 and CeO_2-based composites have gained significant attention as catalysts and as structural and electronic promoters in heterogeneous catalytic reactions.[5] Industrially, cerium oxide is extensively used in three-way catalytic converters for vehicle exhaust treatment,[6] the oxidative coupling of methane, and the water-gas shift reaction.

In this study, we report the synthesis of pure cerium oxide nanoparticles and manganese-doped cerium oxide nanoparticles via the co-precipitation method. The effect of Mn doping on the structural and optical properties of CeO_2 is explored through various characterization techniques.

2. Materials and Synthesis Method

A. Method and Materials

The precursor utilized to make pure ceria NPs and Mn-doped ceria NPs are Cerium nitrate hexahydrate [$Ce(NO_3)_3{\cdot}6H_2O$] and Manganese acetate [$(CH_3.COO)_2Mn.4H_2O$]. The synthesis was carried out by co-precipitation method. Co-precipitation method gives high yield of end product. All of the experimental solutions were prepared with double distilled water containing 10% ethanol.

ISBN: 978-93-95369-55-8 (paperback) 978-93-95369-46-6 (electronic)

Materials Used

- **Cerium Nitrate Hexahydrate** – $Ce(NO_3)_3 \cdot 6H_2O$ Acts as the **cerium precursor**. It provides Ce^{3+} ions necessary for the formation of cerium oxide (CeO_2). It is a highly soluble salt, making it ideal for aqueous synthesis routes.
- **Manganese Acetate Tetrahydrate** – $(CH_3COO)_2Mn \cdot 4H_2O$ Used as the **dopant precursor** to introduce Mn into the ceria lattice. Provides Mn^{2+} ions which can partially substitute Ce^{4+} in the ceria crystal structure, potentially modifying its electronic, structural, and catalytic properties.
- **Solvent** – Double distilled water containing **10% ethanol** ensures high purity of the reaction medium. Ethanol may aid in controlling the particle size and morphology by influencing the nucleation and growth rates.

B. Synthesis Method: Co-precipitation

A Co-precipitation method widely used and straightforward method for synthesizing nanoparticles. This method enables uniform distribution of dopant ions. It Offers a high yield of the end product. Operates under mild conditions, typically at ambient temperature or with moderate heating.

Synthesis Procedure

a) Preparation of Precursor Solutions

- **For pure CeO_2 nanoparticles:** 0.3 M $Ce(NO_3)_3 \cdot 6H_2O$ was dissolved in 50 mL of double distilled water containing 10% ethanol. The solution was stirred thoroughly using a magnetic stirrer.
- **For Mn-doped CeO_2 nanoparticles:** Mn-doping solutions were prepared by dissolving either 0.2 M or 0.3 M of $(CH_3COO)_2Mn \cdot 4H_2O$ in the same solvent system. These were added to the Ce solution for doping, ensuring a homogeneous mixture.

b) Precipitation Process

- **NaOH solution (0.9 M)** was added gradually to the **Ce-only solution** under constant stirring to initiate precipitation. The 0.9 M concentration corresponds to three times the molarity of the Ce precursor, reflecting the stoichiometry of the reaction and the presence of three nitrate ions per Ce^{3+} ion.
- For **Mn-doped systems**, both **NaOH (0.9 M)** and the prepared **Mn solution** were added dropwise and simultaneously to the cerium nitrate solution under continuous stirring. This ensured co-precipitation of cerium and manganese hydroxides.

c) Reaction Chemistry

The reaction occurring in the Ce-only system is:

$$Ce(NO_3)_3\ 6H_2O + 3NaOH \rightarrow Ce(OH)_3 + 3NaNO_3 + 6H_2O$$

ISBN: 978-93-95369-55-8 (paperback) 978-93-95369-46-6 (electronic) | © 2025 Advent Publishing.

- A similar co-precipitation reaction occurs for Mn-doped systems, with Mn^{2+} forming $Mn(OH)_2$ in the process.

d) Aging and Separation

- The resulting suspension was left undisturbed for **24 hours** to allow complete precipitation and formation of a supernatant layer.
- The clear supernatant liquid was **carefully removed using a dropper**.

e) Drying

- The remaining precipitate was transferred to a hot air oven and **dried at 150°C for 3–4 hours** to remove moisture, resulting in dry hydroxide precursors.

f) Grinding

- The dried solid was ground **manually in a mortar and pestle** for several hours until a fine, uniform powder was obtained.

g) Calcination

- The fine powder was **calcined at 300–400°C for 3–4 hours** in a **muffle furnace**.
- During this thermal treatment:
  - The hydroxides were converted to their respective oxides (CeO_2 and Mn-doped CeO_2).
  - The oxidation state of **Ce^{3+}** was transformed to **Ce^{4+}**, forming the stable fluorite-structured CeO_2.
  - Residual organic compounds (e.g., acetate) and moisture were fully eliminated.
  - Calcination temperature was kept well below the melting point of the material to preserve nano-sized features and avoid sintering.

h) Observations

Color Change

- The **pure CeO_2 nanoparticles** exhibited a **light-yellow** color after calcination.
- As the **Mn doping concentration increased**, the nanoparticles' color turned **progressively darker**, indicating successful incorporation of Mn into the ceria matrix and possible changes in oxidation states (e.g., Mn^{2+}, Mn^{3+}, Mn^{4+}) and oxygen vacancy formation.

ISBN: 978-93-95369-55-8 (paperback) 978-93-95369-46-6 (electronic)

3. Nanoparticles Characterization

a) Powder X-ray diffraction

Pure Cerium **Doped Cerium**

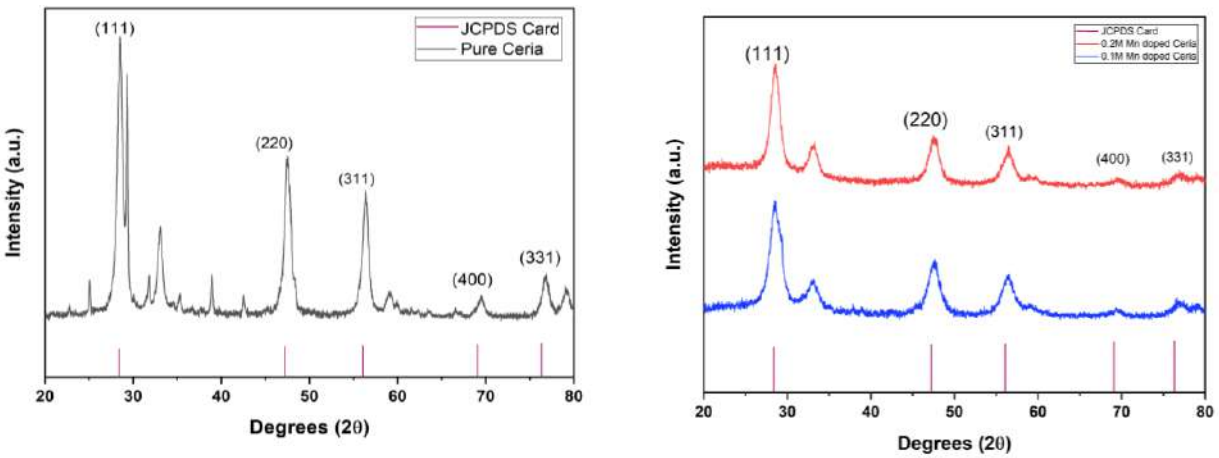

Fig. 1. XRD graph of pure and doped ceria

Powder X-ray diffraction patterns of nanomaterials were recorded using an X-ray diffractometer employing CuK_α radiation. The CuK_α source was operated at 20kV- 40kV. Diffraction data were recorded in a 2θ range from 20° to 80° in 0.02° steps for 0.6 s

The X-ray diffraction (XRD) pattern shown above corresponds to **pure cerium oxide (CeO_2) nanoparticles** synthesized via the co-precipitation method. The diffraction peaks observed at 2θ values of approximately **28.5°, 33.1°, 47.5°, 56.3°, 59.1°, and 69.4°** are indexed to the crystallographic planes **(111), (200), (220), (311), (400), and (331)** respectively. These peaks are in good agreement with the standard data from the **JCPDS card**, confirming that the synthesized nanoparticles possess a **fluorite-type cubic crystal structure**, characteristic of CeO_2. The most intense peak at 28.5° corresponding to the (111) plane indicates that this is the **preferred growth orientation** in the synthesized sample. The sharp and well-defined peaks suggest that the material **is highly crystalline**, with minimal structural defects or amorphous content. Furthermore, the absence of any additional or impurity peaks confirms the **phase purity** of the synthesized CeO_2 nanoparticles. This result confirms the successful formation of pure cerium oxide with desirable crystalline properties, suitable for further modification or application in catalytic and optical materials.

The X-ray diffraction (XRD) pattern shown illustrates the crystalline structure of Mn-doped cerium oxide (CeO_2) nanoparticles at two different doping concentrations: 0.1 M (blue curve) and 0.2 M (red curve). In both samples, prominent diffraction peaks appear at 2θ values of approximately 28.5°,

ISBN: 978-93-95369-55-8 (paperback) 978-93-95369-46-6 (electronic) | © 2025 Advent Publishing.

47.5°, 56.3°, 59.1°, and 69.4°, which correspond to the (111), (220), (311), (400), and (331) planes, respectively. These peaks match well with the standard JCPDS card for fluorite-type cubic CeO_2, indicating that manganese doping does not alter the fundamental crystal structure of cerium oxide. The absence of secondary or impurity peaks confirms that Mn ions are successfully incorporated into the CeO_2 lattice without forming separate manganese oxide phases. A comparison between the two doping levels shows a slight reduction in peak intensity and broadening with increasing Mn content, particularly in the 0.2 M doped sample. This suggests a reduction in crystallite size and possible lattice strain or defect formation, which are typical effects of dopant substitution in the host lattice. The slight broadening of peaks may also indicate increased disorder within the crystal structure due to Mn incorporation. Overall, the XRD analysis confirms that both 0.1 M and 0.2 M Mn-doped CeO_2 nanoparticles maintain a crystalline fluorite structure, with Mn doping subtly influencing the crystallinity and particle size depending on the dopant concentration.

b) Ultraviolet Diffuse Reflectance Spectroscopy (UV-DRS)

UV-diffuse reflectance spectroscopy (DRS) is a type of surface analysis. As a probing medium, it employs ultraviolet (UV) light. Light interacts with "strongly absorbing materials" such as metals, alloys, semiconductors, and so on in the first 10-20 nm.

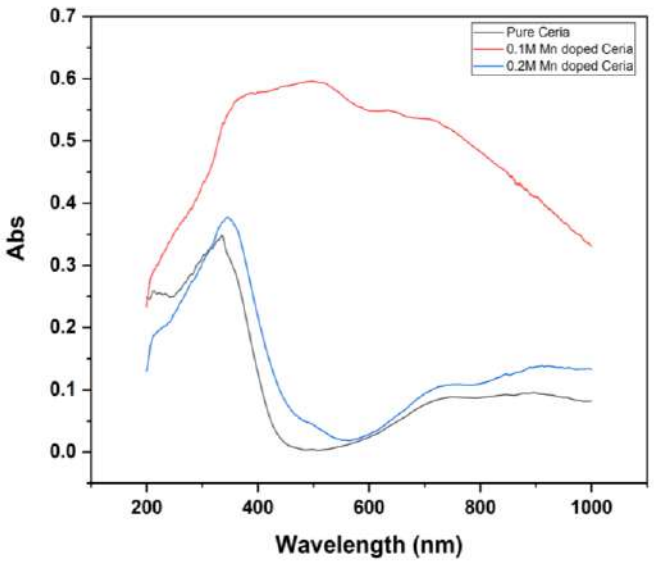

Fig. 2. Absorbance of UV-DRS of pure and doped ceria

The UV–Visible Diffuse Reflectance Spectroscopy (UV-DRS) graph (Fig. 2) presented illustrates the optical absorption behavior of pure cerium oxide (CeO_2) and Mn-doped CeO_2 nanoparticles at two different doping concentrations: 0.1 M and 0.2 M. The absorbance spectra reveal a notable shift in the optical properties as a result of Mn doping. Pure CeO_2 nanoparticles (black curve) show a distinct

ISBN: 978-93-95369-55-8 (paperback) 978-93-95369-46-6 (electronic)

absorption edge in the ultraviolet region, around 380–400 nm, which is typical for CeO_2 with a wide band gap of approximately 3.2 eV. Upon doping with Mn, a significant enhancement in visible light absorption is observed.

The 0.1 M Mn-doped sample (blue curve) exhibits a moderate red shift in the absorption edge, indicating a slight narrowing of the band gap and improved absorption into the visible region. This effect becomes more pronounced in the 0.2 M Mn-doped sample (red curve), which shows a broader and higher absorbance extending further into the visible range (up to ~700 nm), confirming a more substantial reduction in the band gap.

This progressive red shift and increase in absorbance with higher Mn content can be attributed to the introduction of impurity energy levels within the band gap and the formation of oxygen vacancies or defect states, which promote electronic transitions under lower energy (longer wavelength) light. Overall, the UV-DRS results demonstrate that Mn doping effectively enhances the visible light absorption capability of CeO_2 nanoparticles, making them more suitable for applications in photocatalysis, solar energy conversion, and other optoelectronic fields.

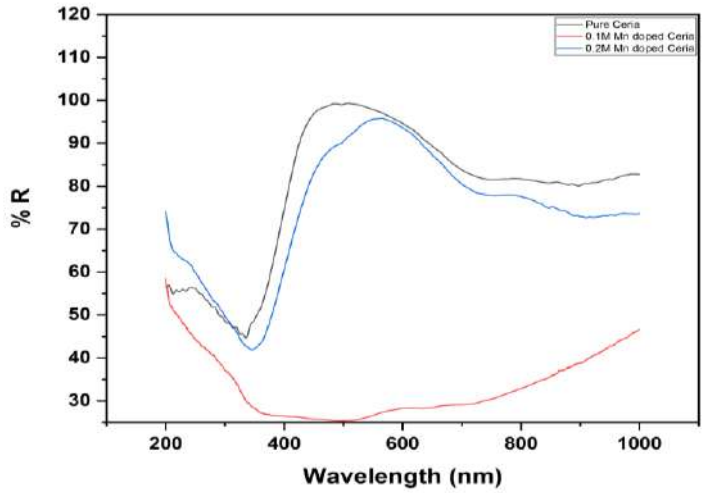

Fig. 3. Reflectance of UV-DRS of pure and doped ceria

The above graph (Fig. 3) shows the UV–Visible Diffuse Reflectance Spectra (UV-DRS) of pure CeO_2 nanoparticles and Mn-doped CeO_2 nanoparticles at 0.1 M and 0.2 M doping concentrations, plotted as % reflectance (%R) vs. wavelength. This reflectance data provides insight into the optical band gap and light interaction behavior of the materials. The pure CeO_2 sample (black curve) exhibits high reflectance in the visible region, particularly between 400 nm and 800 nm, indicating that it absorbs primarily in the UV region and reflects most visible light. This corresponds to its large band gap (~3.2 eV) and limited utility in visible light-driven applications. However, a significant decrease in reflectance is observed in the Mn-doped samples, especially the 0.2 M Mn-doped CeO_2 (red curve), which shows the lowest reflectance

ISBN: 978-93-95369-55-8 (paperback) 978-93-95369-46-6 (electronic) | © 2025 Advent Publishing.

across the entire spectrum. This indicates a higher absorption of light, particularly in the visible region, as Mn doping introduces defect levels or intermediate states within the band gap. The 0.1M Mn-doped sample (blue curve) shows an intermediate behavior, with reflectance lower than that of pure CeO_2 but higher than the 0.2M doped sample. The decrease in reflectance with increasing Mn concentration confirms the enhanced optical absorption due to Mn incorporation, which results in a narrowing of the effective band gap. This enhancement in visible light absorption is consistent with the absorbance data and makes Mn-doped CeO_2 more suitable for photocatalytic and optoelectronic applications, where efficient light harvesting is essential.

c) Field Emission Scanning Electron Microscopy

Field Emission Scanning Electron Microscopy FESEM of nanoparticles were performed by using "NOVA NANOSEM NPEP450". This instrument offers high resolution and excellent contrast, extended accelerating voltage ranging from 50 eV to 30 kV, at wide magnification range. The imaging used various acceleration voltages, beam currents, working distance and aperture setting to obtain the highest resolution possible. The below shows FESEM images of pure and doped ceria.

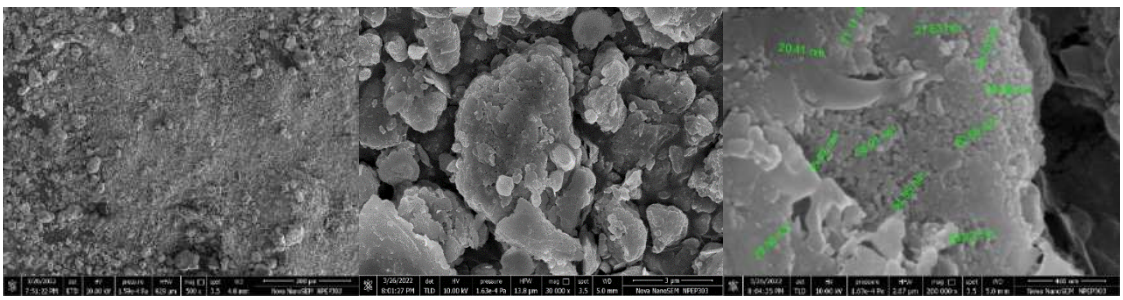

Fig. 4. FESEM of pure cerium

The morphology of pure CeO_2 nanoparticles, as revealed by the FESEM images, shows a **highly aggregated and densely packed structure,** typical for nanoparticles synthesized via the **co-precipitation method**. In the low-magnification image (left), the surface appears rough and granular, suggesting the presence of nanoparticle clusters. As the magnification increases (middle image), more **distinct particle boundaries** become visible. The particles appear to be **irregular in shape**, with rough surfaces and occasional signs of porous regions or voids between aggregates. This suggests that while primary particles are nanoscale, they tend to **agglomerate**, likely due to high surface energy and Van der Waals forces. In the high-magnification image (right), where particle size measurements are provided, the nanoparticles exhibit sizes ranging from approximately **20 to 30 nm**. This nanoscale dimension is consistent with the crystallite size derived from XRD analysis and confirms the **nanostructured nature** of the material. The presence of well-defined but closely packed grains indicates good crystallinity but also suggests some level of **particle coarsening or sintering**, possibly introduced during the drying or calcination steps. Overall, the FESEM images confirm that pure CeO_2 nanoparticles are **polycrystalline, irregularly shaped, and within the nanoscale range**, with a tendency toward agglomeration. This morphology is

ISBN: 978-93-95369-55-8 (paperback) 978-93-95369-46-6 (electronic)

suitable for applications requiring high surface area, such as catalysis, although surface modification or doping (e.g., with Mn) may be required to optimize properties further.

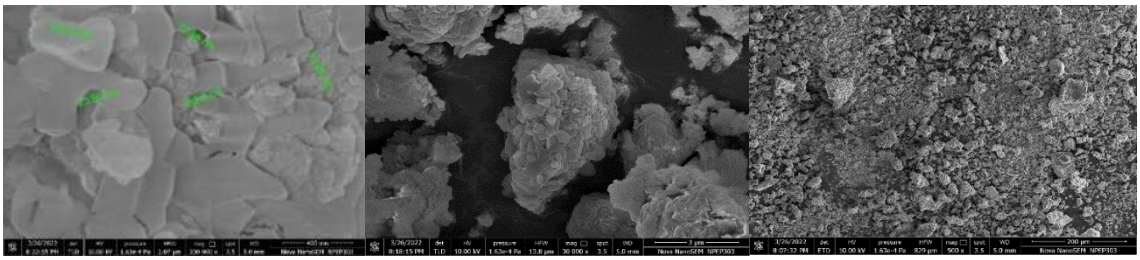

Fig. 5. FESEM of manganese doped cerium

The FESEM micrographs reveal that the Mn-doped CeO_2 nanoparticles exhibit a distinct **morphological evolution** and surface structure compared to pure ceria. In the low-magnification image (top), the particles are aggregated and densely packed, with a somewhat granular surface texture. This aggregation is typical for nanoparticles and can be attributed to their high surface energy and strong interparticle interactions. As the magnification increases (middle image), the particles begin to show more defined and **flower-like or layered structures**, indicating a potential influence of Mn doping on crystal growth patterns and surface energy distribution during synthesis. At the highest magnification (bottom image), the individual particles are clearly visible, and size measurements show nanoparticle dimensions ranging between **20 to 37 nm**. The particles appear **plate-like and closely packed**, with relatively sharp edges, which may suggest a degree of anisotropic growth. The observed size range aligns well with the crystallite sizes estimated from XRD analysis, supporting the nanocrystalline nature of the samples. The incorporation of Mn appears to influence both **particle shape and surface roughness,** potentially enhancing surface area and active sites for photocatalytic or sensor applications. Overall, the FESEM images confirm that **Mn doping alters the surface morphology of CeO_2,** leading to more defined, smaller, and rougher particles compared to pure CeO_2. These structural modifications could significantly impact the optical and catalytic behavior of the nanoparticles.

Applications of Pure and Mn-Doped CeO_2 Nanoparticles

- **Photocatalysis:** Enhanced visible light absorption due to Mn doping makes them suitable for **photocatalytic degradation of pollutants** in water and air purification systems.
- **Solar Energy Conversion:** Improved light absorption properties support their use in **solar cells and photo-electrochemical cells** for energy harvesting.
- **Catalysis:** CeO_2 is widely used in **automotive catalytic converters (three-way catalysts).** Mn doping increases surface area and active sites, enhancing **redox and oxidation reactions.**
- **Sensors:** Their high surface reactivity and conductivity make them ideal for **gas sensing and environmental monitoring**.

ISBN: 978-93-95369-55-8 (paperback) 978-93-95369-46-6 (electronic) | © 2025 Advent Publishing.

- **Fuel Cells:** Used as an **electrolyte material in solid oxide fuel cells (SOFCs)** due to good oxygen ion conductivity and thermal stability.
- **Biomedical Applications:** CeO_2 NPs exhibit **antioxidant properties,** and Mn doping may enhance their use in **drug delivery, imaging, and therapeutic agents.**
- **UV Filters and Protective Coatings:** Pure CeO_2 has strong UV absorption, making it useful in **sunscreens and UV-protective films.**

4. Results and Discussion

The X-ray diffraction patterns confirmed that Mn ions were effectively substituted into the CeO_2 lattice. This observed the diffraction peaks at $2\theta = 28.5°$, 33.1°, 47.5°, 56.3°, and 69.4° correspond to the (111), (200), (220), (311), and (331) planes, respectively. The Mn doping concentration increased, a slight broadening of the peaks and a small reduction in their intensity were observed. This effects confirmed a decrease in crystallite size, lattice strain, and an increase in microstructural disorder, which typically occur due to dopant-induced lattice distortion. Hence **XRD analysis** confirmed the both pure and Mn-doped CeO_2 nanoparticles have a cubic fluorite crystal structure with no secondary phases.

The optical absorption spectra confirmed the notable red shift with Mn incorporation. Pure CeO_2 indicated a sharp absorption edge around 380–400 nm, corresponding to a band gap of around 3.2 eV. Upon Mn doping (0.1 M and 0.2 M), the absorption edge moderately shifted toward longer wavelengths, which indicating a band gap narrowing to the visible region. The increased in absorbance spectra in the region range of 400–700 nm confirms the localized defect states or oxygen vacancies within the band gap and **reflectance** decreased significantly for Mn-doped samples, which enhance visible light absorption. The optical modification induced by Mn doping highlights the material's enhanced suitability for visible-light-driven photocatalytic and optoelectronic applications.

FESEM images confirmed agglomerated, nanosized particles for both pure and doped CeO_2. Pure CeO_2 nanoparticles showed irregular, closely packed grains with particle sizes ranging from 20–30 nm, indicating a tendency toward agglomeration due to high surface energy. In other hand, Mn-doped CeO_2 nanoparticles exhibited more uniform, flower-like and plate-like morphologies with increased surface roughness and reduction of aggregation. This observed particle size for Mn-doped samples ranged from 20–37 nm, consistent with XRD data. The morphological transformation induced by Mn doping suggests modified surface energy and altered crystal growth kinetics during synthesis, which leading to enhanced surface area and potentially improved catalytic performance.

5. Conclusion

This study had successfully synthesized **pure and Mn-doped CeO_2 nanoparticles** via a **co-precipitation method**, achieving nanostructured materials with well-defined crystal structures and enhanced optical properties. Structural analysis confirmed that Mn doping was effectively incorporated into the CeO_2 lattice without altering its cubic fluorite phase. UV-DRS revealed Optical characterization by clear red shift and

ISBN: 978-93-95369-55-8 (paperback) 978-93-95369-46-6 (electronic)

increased visible light absorption with higher Mn concentrations, confirming band gap narrowing. This enhancement in optical response is attributed to the introduction of defect states and oxygen vacancies, which facilitate improved electronic transitions. FESEM reveled Morphological analysis of further validated the nanoscale particle formation and revealed that Mn incorporation modifies the surface texture and reduces agglomeration. The Mn–CeO_2 nanomaterials synthesized here are promising material for various applications, including photocatalysis, solar PV energy conversion, gas sensing analysis, and catalytic processes, due to their enhanced visible light activity and refined nanostructure.

References

1. Bouzigues, Cedric et al. “Biological applications of rare-earth based nanoparticles.” *ACS nano* vol. 5,11 (2011): 8488-505.
2. Dahle, Jessica T, and Yuji Arai. “Environmental geochemistry of cerium: applications and toxicology of cerium oxide nanoparticles.” *International journal of environmental research and public health* vol. 12,2 1253-78. 23 Jan. 2015.
3. Stambouli, A. B. & Traversa, E. Solid oxide fuel cells (SOFCs): a review of an environmentally clean and efficient source of energy. *Renew. Sust. Energ. Rev.* 6, 433–455 (2002).
4. Patil, S., Kuiry, S. C., Seal, S. & Vanfleet, R. Synthesis of nanocrystalline ceria particles for high temperature oxidation resistant coating. *J. Nanopart. Res.* 4, 433–438 (2002).
5. Trovarelli, A. Catalytic properties of ceria and CeO_2-containing materials. *Catal. Rev.* 38, 439–520 (1996).
6. Kaspar, J., Fornasiero, P. & Graziani, M. Use of CeO_2-based oxides in the three-way catalysis. *Catal. Today* 50, 285–298 (1999).
7. Corma A, Atienzar P, García H, Chane-Ching JY. Hierarchically mesostructured doped CeO_2 with potential for solar-cell use. *Nat Mater.* 2004 Jun; 3(6):394-7.
8. Celardo, I., Pedersen, J. Z., Traversa, E. & Ghibelli, L. Pharmacological potential of cerium oxide nanoparticles. *Nanoscale* 3, 1411–1420 (2011).
9. S. Beena, Nelsa Abraham, V. Suresh Babu, Facile synthesis and characterization studies of Mn Co-doped ceria nanoparticles: A promising electrode material for supercapacitors, *Materials Today: Proceedings*, 2021

ISBN: 978-93-95369-55-8 (paperback) 978-93-95369-46-6 (electronic)